Journal of Physics: Conference Series **2889** (2024) 012020 doi:10.1088/1742-6596/2889/1/012020

# Robust design and performance of NPL Cs fountain clocks

**K Szymaniec[1], R J Hendricks[1], J Whale[1], A Wilson[1], S Walby[1,2], M Knapp[1], C J Foot[2]**

[1]National Physical Laboratory, Teddington, UK
[2]Department of Physics, University of Oxford, Oxford, UK

email: krzysztof.szymaniec@npl.co.uk

**Abstract**
We report on developments in the atomic fountain systems being built and operated at NPL. An improved generation of Cs fountains has been developed, with units being constructed for use by both NPL and commercial customers. These systems combine world-class stability and accuracy with increased reliability and can run for long periods of time without maintenance. Here we describe how the NPL fountains work, and present performance data for the latest systems. We describe some of the applications of these fountains, both in time scale implementation and fundamental science. We also present an overview of a miniature atomic fountain that is being developed, which will help make fountain technology accessible to a wider range of sectors.

## 1. Introduction

Atomic fountain clocks have become ubiquitous in maintaining the most stable national time scales within a small margin of UTC and, as primary or secondary frequency standards, have the dominant role in the computation of the TAI time scale. A number of national measurement institutes and other labs have pursued their development, reaching accuracy close to only one part in $10^{16}$ (for recent evaluation reports see, for example, [1][2][3]). After three decades of effort and many improvements the designs of fountain clocks have reached a high level of maturity and recent work has been aiming towards increased robustness and reliability.

At NPL we have adopted a distinctive design approach offering the highest accuracy and best short-term stability, yet with relatively simple construction and operation. With the confidence gained from several years of operation of NPL-CsF2, the approved primary frequency standard for the UK [4][5], we have designed an upgraded version of the fountain, which was subsequently offered and delivered to customers under the rigour of commercial contracts. Devices have been constructed and sent to other national measurement institutes, large scientific facilities, and potential future customers include providers of telecommunication and financial services.

In this presentation we review the key features of the NPL design (section 2) and the performance of selected realisations of the clocks (section 3). We also refer to a technique for further accuracy improvement by limiting a leading cause of systematic bias, the distributed cavity phase effect. Implementation of the highly reliable fountain clocks to steer a local time scale is covered in section 4. Finally, in section 5, we present the concept of *mini-fountain*, a compact version of the clock, which aims to achieve comparable performance to the NPL fountains but with much reduced size of the physics package and other subsystems including the optical bench.

## 2. Features of the NPL Cs fountain design

The general features of fountain clocks are replicated in the majority of working devices [6][7]. Laser cooled atoms are collected and launched vertically in a cloud with a temperature of a few microkelvin. On both ascent and descent, they pass through a microwave cavity that is resonant with the clock transition between the hyperfine sublevels of the ground state atoms. The two interactions with microwaves in the cavity separated by the field-free period constitute a Ramsey interrogation scheme, with a typical Ramsey fringe width of about 1 Hz. Laser induced fluorescence signals from a two-zone time-of-flight detection region enable direct inference of normalised probability of the clock transition.


**Figure 1.** View of the 'full size' physics package of the improved NPL Cs fountain design. *Left:* drawing showing the layout and main functional regions (C-field coil and magnetic shields are not shown). *Right:* photograph of an assembled unit.

The variations between different fountain designs generally relate to how the cold atoms are produced and prepared in a suitable state for the interrogation. Furthermore, various approaches are used to control systematic effects such as cold collisions, blackbody radiation, microwave leakage or distributed cavity phase effects. The specific features of the NPL design are summarised below and more details can be found in [8]. See also fig. 1 for the illustration of the physics package.

- The cold caesium atoms are initially collected and cooled in a single-stage vapour-loaded magneto-optical trap (MOT), using an easy to align (0,0,1) optical configuration. The vapour is produced by a temperature controlled (cooled) reservoir of caesium metal.
- After the MOT fields are switched off the initial atom cloud size is tuned with a short and variable period of expansion before the subsequent phase of molasses cooling.
- The population of the initial clock state (F=4, $m_F$=0) is boosted by an optical pumping (OP) pulse [9] applied in an additional light access area between the MOT and detection chambers. The pulse is derived from the cooling laser and tuned to the ($F$=4 → $F'$=4) component of the D2 transition. A pulsed magnetic field from a pair of small Helmholtz coils defines the quantisation axis for the linear π polarisation of the OP light. This technique increases the detection signal approximately five-fold, which is an optimum between a higher spin polarisation and heating due to random scattering of photons resulting in truncation of the cloud.
- The microwave cavity assembly consists of two cavities, with the lower one used for the usual clock state purification, which is necessary due to the limitations of the OP method used. The

upper one is the Ramsey cavity specially designed to minimise the distributed cavity phase effect [10]. The atoms' flight above the Ramsey cavity is entirely enclosed in a narrow tube that forms a waveguide below cut-off and prevents their exposure to any leaked resonant microwave field.

- The chamber housing the cavities assembly and the flight tube is built with a double wall water jacket, which is used to control the temperature of this area. This helps to finely tune the Ramsey cavity to the atomic (clock) resonance as well as to improve the uniformity of the temperature of the surroundings and the resulting blackbody radiation.
- The detection chamber is designed to maximise the solid angle of the fluorescence collection with retroreflectors nearly doubling the time-of-flight signal. In addition, the laser beams inducing the fluorescence are tilted by 10° from the horizontal to reduce resonant scattering by the thermal background by means of the Doppler effect [11]. The intensity of these beams is stable to 0.1%

The complete system, including the physics package, can be transported fully assembled by road or air. Subsystems, such as control electronics, microwave generation and optical bench are all mounted in just two full height 19-inch racks. The optics (including lasers) are built in a modular way and entirely mounted in one of the racks without need for an optical table. They incorporate a distributed Bragg reflector (DBR) type diode laser for cooling and detection and a distributed feedback diode (DFB) as repump laser.

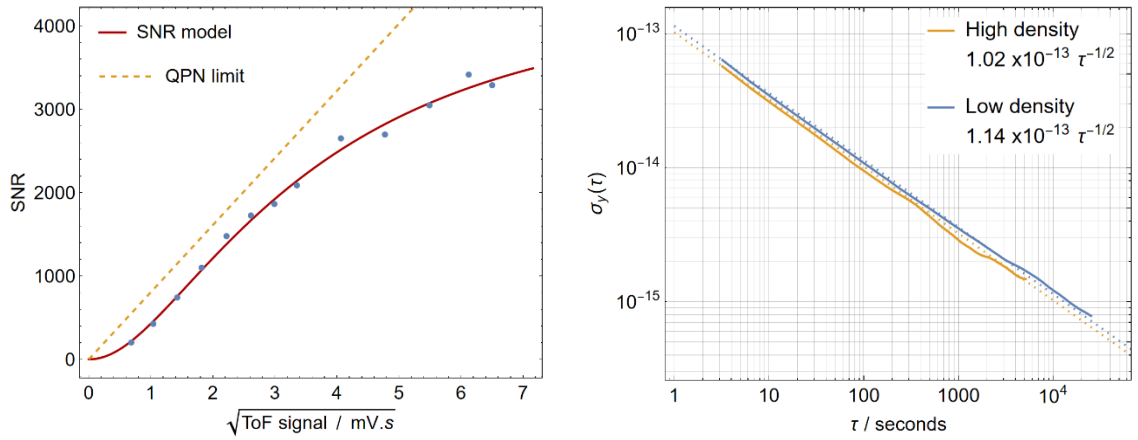


**Figure 2.** *Left:* Measurements of fountain signal-to-noise ratio (SNR) as a function of the square root of the atom density, showing SNR values in excess of 3000. The fitted SNR model enables us to estimate the effect of quantum projection noise (QPN) and shows that this, rather than technical noise, is dominant except at very high and low atom number. *Right:* Measurements of the short-term stability at high and low atom density when operating with a quartz local oscillator. The very similar stability for different densities indicates that the measurement is limited by the local oscillator noise.

## 3. Performance

The combination of launching from a MOT and using the optical pumping technique enables the NPL fountains to operate with a large number of detected atoms. Together with optimised detection, which reduced technical noise, this leads to an excellent signal-to-noise ratio (SNR) that is largely dominated by the quantum projection noise due to the atoms being detected in a superposition of the clock states (fig. 2). Using a low phase noise local oscillator (LO) based, for example, on a cryo-cooled sapphire crystal or on a femtosecond frequency comb locked to an ultra-stable laser, the corresponding short-term stability $\sigma_y(\tau)$ of the fountain would be in the range of $3\times10^{-14}$ at $\tau = 1$ s integration time. When used with an LO based on a room temperature quartz crystal, which has worse phase noise, we observe that the stability is degraded to $\sigma_y(\tau)$ of $1.0\times10^{-13}$ (1 s). For maximum accuracy the atom number (density) must be alternated between high and low, and the measured frequency is extrapolated to zero

density. This further degrades the effective short-term stability by up to a factor 3, depending on the LO properties [12].

For accuracy evaluations with low uncertainty as well as for the day-to-day operation of the fountain clock, both a good SNR and a high uptime are required. To improve the latter, we have identified key failure cases, such as, the laser frequency stabilisation, the system control software, temperature control of the flight tube and caesium reservoir, and durability of mechanical shutters on the optical bench. Upon addressing the operational robustness in these cases, the NPL built fountains have demonstrated operation over several months without any unintentional stoppages. NPL-CsF2 has routinely reached uptime of 99%, as measured monthly when not limited by the availability of the microwave signal being measured.

An illustrative uncertainty budget for a fountain clock of the NPL design is given in table 1. The type B values presented are the typical or expected values taken from previous evaluations and measurements, leading to the total uncertainty $u_B$ of below $2\times10^{-16}$. This is similar to the best fountains currently approved for reporting of data to TAI [1].

| Systematic effect | uncertainty /$10^{-16}$ |
|---|---|
| 2nd order Zeeman | 0.4 |
| Blackbody radiation | 0.7 |
| Cold collisions | 0.3 |
| Background gas | 0.3 |
| Microwave leakage | 0.6 |
| Distributed cavity phase | 1.1 |
| Microwave lensing | 0.3 |
| Other | 0.4 |
| **Total $u_B$** | **<2** |

**Table 1.** Values of type-B uncertainties compiled from previously published evaluations [refs NPL, NRC, AOS]. The values shown present an illustrative budget of the accuracy currently achievable by the NPL-built Cs fountain primary frequency standards. Implementation of our new DCP evaluation technique will further improve the accuracy of the system.

Historically, the frequency shift due to cold collisions had been one of the limiting factors in the accuracy of Cs fountain primary frequency standards. Here, this shift is virtually eliminated by tuning the effective collisional energy and adjusting the clock states ratio between the Ramsey interactions [13]. This is achieved despite loading the atoms in the MOT, launching them in a small high-density cloud and implementing the OP stage which largely preserves the high density. As described above, the residual collisional shift must still be corrected for by measuring at both high and low atom densities [12].

In the budget presented in table 1 the largest uncertainty is associated with the distributed cavity phase (DCP) effect, which is essentially a Doppler shift caused by travelling wave components of the microwave field in the cavity. The established treatment follows [14] where these components are approximated as the lowest order terms of an azimuthal series, $m = 0, 1, 2$. It can be shown that the $m = 1$ and $m = 2$ terms may lead to a negligible frequency shift if the atomic trajectories precisely retrace the cavity crossing positions on ascent and descent. Using conventional approaches to optimising the atomic trajectories, the frequency uncertainty introduced by the DCP effect can be limited to about $1\times10^{-16}$. Following on an earlier work [15] we have developed a technique to precisely determine the crossing positions of the centre of mass of the ensemble of atoms that contribute to the detection time-of-flight signal. The technique uses the approximately linear variation of the transverse components of the cavity

field, and we were able to detect and centre the crossing positions to better than 50 μm, which can limit the DCP shift and its uncertainty to less than $1\times10^{-17}$ [16].

## 4. Applications

The main motivation for the development of atomic fountains was their potential use as primary or secondary frequency standards and, indeed, for the last two decades they have been the dominant source of accuracy for the international time scale UTC [17]. Another related application is as a frequency reference for ultra-high precision spectroscopy measurements, an example being the ALPHA experiment on antihydrogen [18] or measurements of frequency ratios between the clock transitions in Cs and candidate transitions for optical clocks [19][20], the latter leading to constraints on fundamental constants variations, especially on the electron-to-proton mass ratio [21].

While for PFS operation intermittent availability of a fountain is adequate, with their significantly improved reliability they can now operate quasi-continuously, and it is possible to utilise them as a resource enhancing the stability of local UTC time scales. Over the last 5 years, we have used the high availability of the NPL-CsF2 fountain and provided regular and frequent steering corrections for the UTC(NPL) master clock (a hydrogen maser). The fountain's long-term stability is significantly better than that of any maser hence it is sufficient to use a relatively simple algorithm for the steering process where the frequency of the reference clock is acted upon (not the phase). It consists of two components, a frequency feedback loop, and a phase lock loop [22][23]. The first component comes from a direct measurement of the reference maser frequency with an added term due to its anticipated linear drift. The drift is also determined by the fountain, but over a longer period of 2 months. For the phase lock component, the high uptime of the fountain is even more important as it effectively acts as a holdover clock. This term additionally includes a correction for an accumulated time offset between UTC and UTC(NPL) due to imperfect steering during the preceding latency period. Fig. 3 shows the exemplary performance of UTC(NPL) prediction over a typical BIPM reporting period with an added latency.

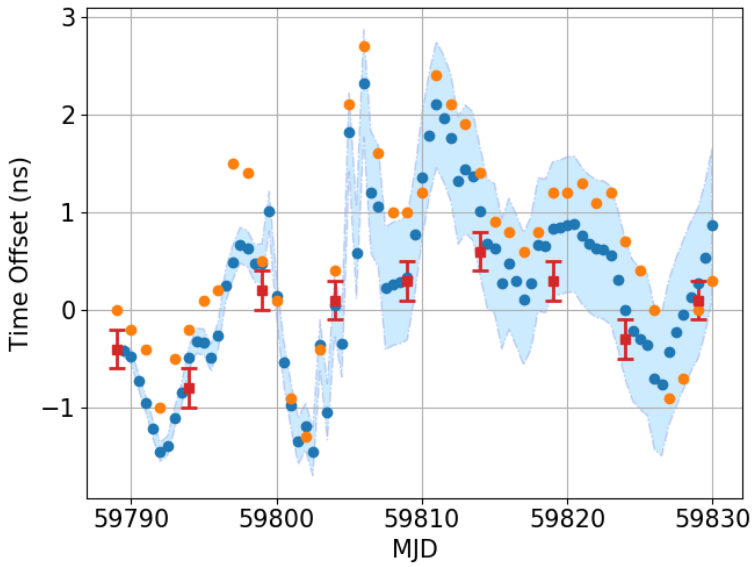


**Figure 3.** Time offset of UTC(NPL) from UTC as estimated in real time by Cs fountain NPL-CsF2 (blue points). The method's capability is illustrated by a data set when a less stable maser was used as the reference for UTC(NPL). The first point is obtained from the preceding month's Circular T, and the shaded region shows the uncertainty of this estimate as the time progresses. Also plotted are subsequent UTCr (orange circles) and UTC data (red squares), which arrive with a latency of up to 10 and 45 days, respectively.

Operational time scales typically use hydrogen masers as flywheel oscillators to cover any gaps in the frequency standards' availability. To reduce the phase noise on the maser reference signal and the corresponding degradation of the fountain short-term stability a clean-up oscillator is implemented (see above sec 3 and fig. 2). We have recently acquired a cryo-cooled sapphire oscillator (CSO) and have investigated its application not only as a clean-up but also as a flywheel, that is, its stability in long term. We have observed substantial CSO linear frequency drift but noticed that it is highly predictable and can be efficiently removed in a feed-forward loop. With such correction in place, it should be possible to operate a time scale with a CSO as reference, which could be disciplined directly by a Cs fountain (without a need for a maser in the system). The flicker floor of a corrected CSO would be at the level of $10^{-15}$, fractionally, such that the typical gaps in fountain operation of a few hours or a day could be tolerated.

## 5. Mini-fountain concept

In the preceding sections we have described the optimised design and applications of a 'full size' caesium fountain clock, which achieves the best stability, accuracy, and reliability. The mini fountain concept (*mini-f*) described in this section is driven by the needs of industrial users and service providers for a time scale realisation which would be stable to several nanoseconds over up to 6 weeks, the latency period of UTC feedback. The key design requirement is to reduce as much as practical the size, weight and power consumption (SWaP), complexity, and cost, while achieving similar performance to a fountain clock operating with a quartz-based local oscillator, i.e. short-term stability of $3\times10^{-13}$ (1 s), and in the long-term better than $1\times10^{-15}$. The ability to independently characterise the accuracy (systematic frequency shifts), as in primary or secondary frequency standards, should be possible but is not essential.

Fountain technology appears well suited to meet these requirements, provided appropriate design choices are made. For example, while reducing the overall size of the physics package, we would leave unchanged the actual fountain height (distance from the cavity centre to the atomic trajectory apex) and hence the clock linewidth. The Ramsey cavity would be sealed as part of the vacuum vessel and the magnetic shielding would only have two layers. Importantly, there would be no separate detection chamber or state selection cavity. A simple antenna emitter would be used for the state selection and the unselected $m_F \neq 0$ population would be removed by a pulse from the downwards-going cooling beams.

The final clock states' populations will be detected by the same beams used for the initial trapping and cooling. A new normalised detection method will be implemented as shown in fig. 4a. First, as the descending cloud reaches the MOT region, a pulse from all six cooling beams induces fluorescence only from the population of the 'upper' clock state, $N_u$, which decays as the atoms are off-resonantly pumped to the 'lower' clock state, which only couples to the repump, with the initial population $N_l$. Next, a short repump pulse puts all the atoms in the upper state. This is followed by another cooling beam pulse, which induces a second fluorescence signal proportional to $N_{tot} = N_l + N_u$. Alternatively, the repump pulse can be combined with the second cooling pulse, as would be necessitated by the use of an EOM for generation of repumping light. A substantial background fluorescence, resulting from the atomic vapour present in the MOT chamber, is measured and subtracted after one more cooling pulse, delayed so that the cold atoms do not contribute. The clock transition probability is directly obtained as $P = N_u/N_{tot}$.

We have tested the new detection scheme in a simple cold atom source demonstrator and in our experimental fountain setup NPL-CsF3. The scheme was shown to work robustly, and preliminary results are shown in fig. 4b. The high-atom-number limit to the SNR was found to be around 800, limited by laser noise. However, at an atom number corresponding to a typical MOT loading time ($N_{at} \approx 0.5$ a.u.), the SNR is limited by technical noise to only around 100. This noise can be reduced with a purpose-designed cooling/detection chamber, where the fluorescence collection solid angle is optimised, such that we anticipate a detection signal-to-noise ration of around 500. The tests were performed on Cs,

however, in the actual mini-f clock we plan to use $^{87}$Rb to increase the clock-state population without the need for optical pumping, as well as to reduce effects arising from the cold-collision frequency shift.

Performing the detection in the trapping chamber will also simplify the optical bench as no separate detection beams will be needed. Furthermore, for compactness, we will use all fibre-coupled optics, especially where alignment is critical. Only one stabilised narrowband laser will be necessary for cooling and the repump light will be generated by an electro-optic modulator sideband; a tapered amplifier will boost the light intensity to the level necessary for efficient trapping and cooling.

The mini-f physics package is shown in fig. 4c and has been designed in-house. It will have a volume of 25 litres, which is about 30 times smaller than that of the 'full-size' fountain. The design also includes a microwave cavity with a bent waveguide to feed the cavity symmetrically from a single cable source (based on a design by [24]). The waveguide will be on the airside, while the cavity will be under vacuum and sealed by dielectric viewports added over the coupling holes between the waveguide and the cavity. The remaining subsystems such as the optics, microwave synthesizer and control electronics will utilise commercial-off-the-shelf solutions to accelerate the development.

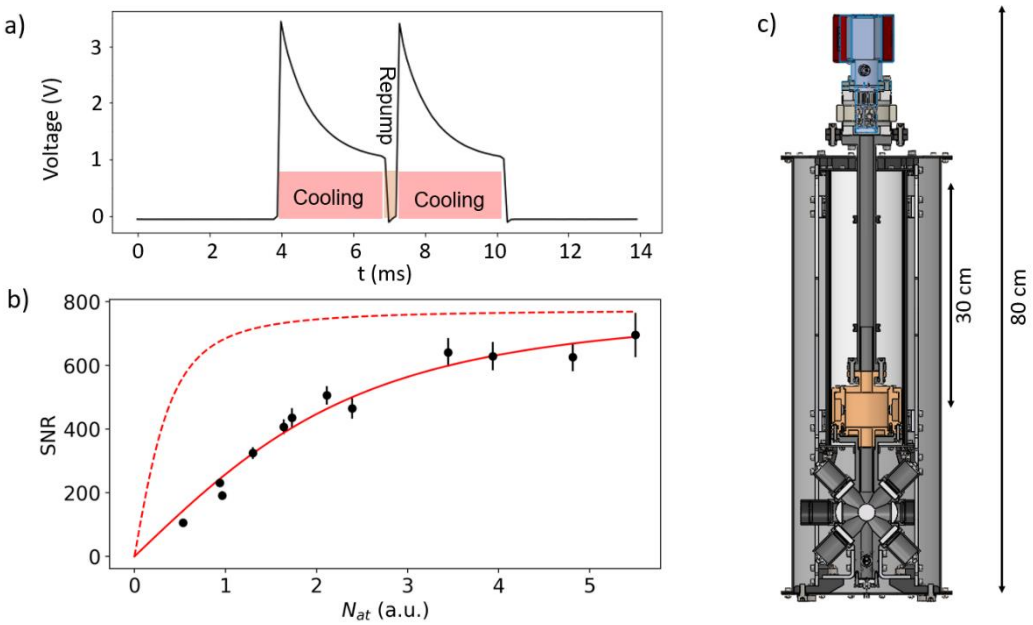


**Figure 4.** a) Detector output voltage as a function of time for the detection pulse sequence. b) Signal-to-noise ratio vs atom number measured in experiments in CsF3 (data points, solid curve), and expected for improved fluorescence collection in a custom-designed cooling/detection chamber (dashed curve). c) Diagram of the mini-f prototype physics package.

## 6. Conclusions

We have reviewed the development and performance of the Cs fountain primary frequency standards built by NPL, including several units delivered under commercial contracts. Despite a simple design, the fountains are capable of achieving the best performance in terms of short-term stability and type-B uncertainty as compared to values reported by other groups. Furthermore, the uncertainty of DCP, one of the largest systematic effects, typically evaluated at $1\times10^{-16}$ following conventional methods, can be reduced 10-fold with a technique requiring only a minor modification to the physics package.

We note that further improvements of the accuracy of fountain clocks by reducing uncertainties of other systematic effects would be increasingly difficult to achieve. This is, on one hand, due to a limited

ability to model some of these effects (e.g. blackbody radiation shift) and, on the other hand, because there is no clear path to further improve the short-term stability and reduce the averaging time needed to reach a given level of the frequency measurement resolution.

This implies that development effort is now better spent on improving the reliability of fountain clocks. The high uptime, above 99%, that we have demonstrated allows us to use the atomic fountain as a holdover clock for periods between Circular T publications or longer. It should also be possible to use a CSO as a flywheel oscillator without a need for a hydrogen maser.

Improved reliability and simplicity of operation makes it possible to run fountain clocks outside of laboratory environments. NPL is making use of this feature to build a more resilient time scale with infrastructure distributed across multiple locations [25]. More robust atomic fountains also open up applications in a wider range of sectors, such as telecoms and financial services. This is even more true of the mini-fountain, which promises to bring the benefits of compactness, simplicity, and affordability.

**Acknowledgments**

We are grateful to Kurt Gibble for stimulating discussions and to Kathryn Kathry, Filip Ozimek and Peter Lovelock for technical contributions at various stages of this work. We also acknowledge Peter Whibberley for critical reading of the manuscript.

**References**

[1] Weyers S, Gerginov V, Kazda M, Rahm J, Lipphardt B, Dobrev G and Gibble K 2018 *Metrologia* **55** 789

[2] Beattie S, Jian B, Alcock J, Gertsvolf M, Hendricks R, Szymaniec K and Gibble K 2020 *Metrologia* **57** 035010

[3] Wang X-L *et al.* 2023 *Metrologia* **60** 065012

[4] Li R, Gibble K and Szymaniec K 2011 *Metrologia* **48** 283

[5] Szymaniec K, Lea S N, Gibble K, Park S E, Liu K and Głowacki P 2016 *J. Phys.: Conf. Ser.* **723** 012003

[6] Wynands R and Weyers S 2005 *Metrologia* **42** S64

[7] Guéna J *et al* 2012 *IEEE Trans. UFFC* **59** 391

[8] Hendricks R J, Ozimek F, Szymaniec K, Nagórny B, Dunst P, Nawrocki J, Beattie S, Jian B and Gibble K 2019 *IEEE Trans. UFFC* **66** 624

[9] Szymaniec K, Noh H-R, Park S E, Takamizawa A 2013 *Appl. Phys. B* **111** 527

[10] Gibble K, Lea S N and Szymaniec K 2012 *Proc. Conference on Precision Electromagnetic Measurement (Washington DC, USA)* 700

[11] Laurent Ph *et al.* 2006 *Appl. Phys. B* **84** 683

[12] Szymaniec K, Park S E 2011 *IEEE Trans. Meas. Instrum.* **60** 2475KS+SEP IEEE 2012

[13] Szymaniec K, Chałupczak W, Tiesinga E, Williams C J, Weyers S and Wynands R 2007 *Phys. Rev. Lett*. **98** 153002

[14] Li R and Gibble K 2010 *Metrologia* **47** 534

[15] Nemitz N, Gerginov V, Wynands R and Weyers S 2012 *Metrologia* **49** 468

[16] Burrows K, Hendricks R J, Szymaniec K, Gibble K, Beattie S and Jian B 2020 *Metrologia* **57** 065003

[17] BIPM Time Department Database *https://webtai.bipm.org/database/show_psfs.html*

[18] Madsen N 2021 *Europhys. News* **52** 18

[19] Godun R M, Nisbet-Jones P B R, Jones J M, King S A, Johnson L A M, Margolis H S, Szymaniec K, Lea S N, Bongs K and Gill P 2014 *Phys. Rev. Lett.* **113** 210801

[20] Lange R, Huntemann N, Rahm J M, Sanner C, Shao H, Lipphardt B, Tamm Ch, Weyers S and Peik E 2021 *Phys. Rev. Lett.* **126** 011102

[21] Barontini G *et al.* 2022 *Eur. Phys. Journal Quantum Tech.* **9** 12
[22] Rovera G D, Bize S, Chupin B, Guéna J, Laurent Ph, Rosenbusch P, Uhrich P and Abgrall M 2016 *Metrologia* **53** S81
[23] Galleani L, Signorile G, Formichella V and Sesia I 2020 *Metrologia* **57** 065015
[24] Schröder R, Hübner U and Griebsch D 2002 *IEEE Trans. UFFC* **49** 383
[25] Jones D J M *et al.* 2024 (submitted to this issue)